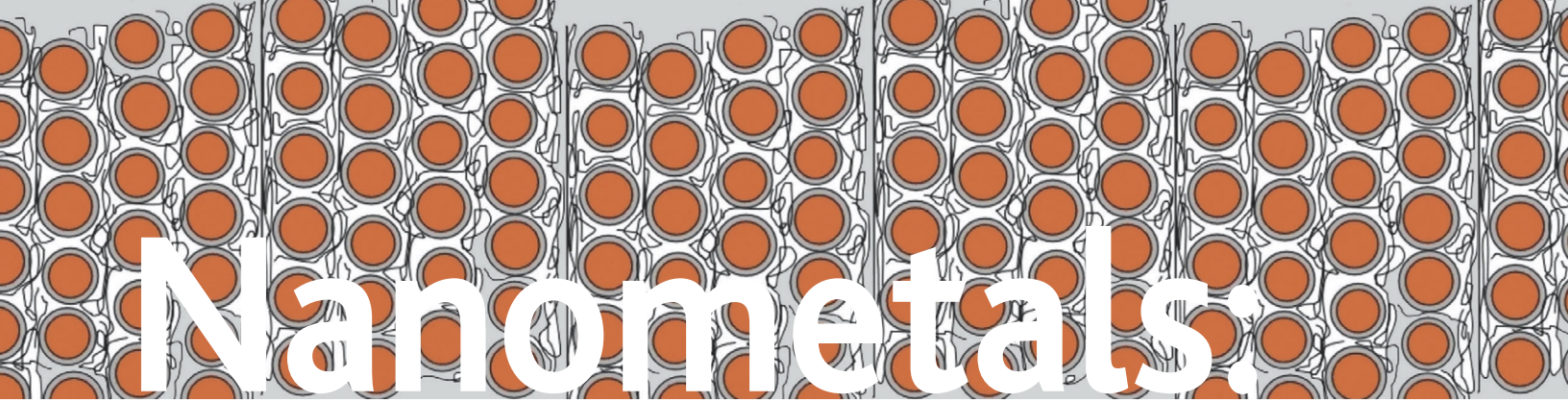

Nanometals: formation and color

by Luis M. Liz-Marzán

Metal nanoparticles are very attractive because of their size- and shape-dependent properties. From the plethora of existing procedures for the synthesis of metal nanoparticles, the most widely used wet-chemical methods are briefly discussed, which are suitable for production of both spherical and anisometric (rod-like or prismatic) nanoparticles. The optical properties of these nanoparticles are spectacular and, therefore, have promoted a great deal of excitement during the last few decades. The basics of the origin of such optical properties are described and some of the theoretical methods accounting for them are briefly presented. Examples are shown of the color variations arising from changes in the composition, size, and shape of nanoparticles, as well as from the proximity of other metal nanoparticles.

Departamento de Quìmica Fìsica,
Universidade de Vigo,
36200 Vigo, Spain
E-mail: lmarzan@uvigo.es
URL: webs.uvigo.es/coloides/nano

Nanotechnology, nanoscience, nanostructures, nanoparticles... These are now some of the most widely used terms in materials science literature. But why are nanoscale materials and processes so attractive? From the point of view of the general public, nanotechnology appears to be the fabrication of miniature machines, which will be able to travel through the human body and repair damaged tissues, or supercomputers small enough to fit in a shirt pocket. However, nanostructured materials have potential applications in many more areas, such as biological detection, controlled drug delivery, low-threshold lasers, optical filters, and sensors, among others.

In fact, it is relatively easy to find examples of the use of metal nanoparticles (maybe not deliberately) as decorative pigments since the time of the Romans, such as those contained in the glass of the famous Lycurgus Cup (4th century AD). The cup can still be seen at the British Museum[1] and possesses the unique feature of changing color depending upon the light in which it is viewed. It appears green when viewed in reflected light, but looks red when a light is shone from inside and is transmitted through the glass. Analysis of the glass reveals that it contains a very small amount of tiny (~70 nm) metal crystals containing Ag and Au in an approximate molar ratio of 14:1. It is the presence of these nanocrystals that gives the Lycurgus Cup its special color display.

It was not until 1857, however, that Michael Faraday reported a systematic study of the synthesis and colors of

ISSN:1369 7021 © Elsevier Ltd 2004

colloidal gold[2]. Since that pioneering work, thousands of scientific papers have been published on the synthesis, modification, properties, and assembly of metal nanoparticles, using a wide variety of solvents and other substrates. All this has led not only to reliable procedures for the preparation of metal nanoparticles of basically any desired size and shape, but also to a deep understanding of many of the physico-chemical features that determine the characteristic behavior of these systems.

One of the most interesting aspects of metal nanoparticles is that their optical properties depend strongly upon the particle size and shape. Bulk Au looks yellowish in reflected light, but thin Au films look blue in transmission. This characteristic blue color steadily changes to orange, through several tones of purple and red, as the particle size is reduced down to ~3 nm. These effects are the result of changes in the so-called surface plasmon resonance[3], the frequency at which conduction electrons oscillate in response to the alternating electric field of incident electromagnetic radiation. However, only metals with free electrons (essentially Au, Ag, Cu, and the alkali metals) possess plasmon resonances in the visible spectrum, which give rise to such intense colors. Elongated nanoparticles (ellipsoids and nanorods) display two distinct plasmon bands related to transverse and longitudinal electron oscillations. The longitudinal oscillation is very sensitive to the aspect ratio of the particles[4], so that slight deviations from spherical geometry can lead to impressive color changes. Apart from single particle properties, the environment in which the metal particles are dispersed is also of relevance to the optical properties[5]. The refractive index of the surrounding medium[6], as well as the average distance between neighboring metal nanoparticles[7], has been shown to influence the spectral features, as will be described below.

Synthesis of metal nanoparticles

In this short review, we do not have the scope to describe all the existing methods for the preparation of metal nanoparticles. This section will be restricted, therefore, to some of the most widely used methods based on chemical reactions in solution (often termed 'wet chemistry') that yield metal nanoparticle colloids.

Probably the most popular method of preparing Au nanospheres dispersed in water is the reduction of $HAuCl_4$ in a boiling sodium citrate solution[8,9]. The formation of uniform Au nanoparticles is revealed by a deep wine red color observed after ~10 minutes[10]. The average particle diameter can be tuned over quite a wide range (~10-100 nm) by varying the concentration ratio between the Au salt and sodium citrate[9]. However, for particles larger than 30 nm, deviation from a spherical shape is observed, as well as a larger polydispersity. The same procedure can be used to reduce an Ag salt, but particle size control is very limited. Citrate reduction has also been applied to the production of Pt colloids of much smaller particle sizes (2-4 nm), which can be grown further by hydrogen treatment[11,12].

Another procedure that has become extremely popular for Au nanoparticle synthesis is the two-phase reduction method developed by Schiffrin and coworkers[13,14]. Basically, $HAuCl_4$ is dissolved in water and subsequently transported into toluene by means of tetraoctylammonium bromide (TOAB), which acts as a phase transfer agent. The toluene solution is then mixed and thoroughly stirred together with an aqueous solution of sodium borohydride (a strong reductant), in the presence of thioalkanes or aminoalkanes, which readily bind to the Au nanoparticles formed. Depending on the ratio of the Au salt and capping agent (thiol/amine), the particle size can be tuned to between ~1 nm and ~10 nm. Several refinements of the preparative procedure, including the development of analogous methods for the preparation of Ag particles, have been reported[15,16]. Murray and coworkers have enhanced the method's popularity by offering an interesting and elegant alternative to the two-phase reduction method, which has opened a new field of preparative chemistry. They explored routes to functionalized monolayer-protected clusters by ligand place exchange reactions[17,18].

Several examples exist of the reduction of metal salts by organic solvents. Ethanol has been long used for the preparation of metal nanoparticles such as Pt, Pd, Au, or Rh (suitable for catalytic applications) in the presence of a protecting polymer, usually poly(vinyl pyrrolidone) or PVP[19,20]. Another important example is found in Figlarz's polyol method, which consists of refluxing a solution of the metal precursor in ethylene glycol or larger polyols[21,22]. Xia and coworkers recently demonstrated that the polyol method can be applied to the production of Ag nanowires and nanoprisms by reducing $AgNO_3$ with ethylene glycol in the presence of PVP[23,24]. Ag nanoparticles with high aspect ratios were only grown in the presence of (Pt) seeds formed *in situ*

prior to the addition of the Ag salt. The dimensions of the Ag nanowires can be controlled by varying the experimental conditions (temperature, seed concentration, ratio of Ag salt and PVP, etc.). On the other hand, Liz-Marzán and coworkers have reported the ability of N,N-dimethylformamide (DMF) to reduce Ag^+ ions, so that stable spherical Ag nanoparticles can be synthesized using PVP as a stabilizer[25]. In addition, SiO_2- and TiO_2-coated nanoparticles[26,27] can be produced by the same method, in the presence of aminopropyl-trimethoxysilane and titanium tetrabutoxide, respectively. Interestingly, the shape (and size) of the nanoparticles obtained in this way depends on several parameters, such as Ag salt and stabilizer concentrations, temperature, and reaction time. Specifically, when PVP is used as a protecting agent, spherical nanoparticles form at low $AgNO_3$ concentrations (<1 mM)[25], while increasing Ag concentration (up to 0.02 M) largely favors the formation of anisotropic particles[28,29]. Again, the concentration of PVP and the reaction temperature strongly influence the shape of the final particles.

As mentioned above, deviations from spherical geometry strongly affect the optical properties of metal nanoparticles. For this reason, methods for the synthesis of anisometric nanoparticles in solution (nanorods, nanowires, nanodisks, nanoprisms, etc.) are continuously being reported, in particular for Au[30-33] and Ag[34-36]. Some of these are described in the previous paragraph, but others deserve a brief description as well.

The first method for synthesis of Au nanorods in solution (electrochemical growth within inorganic templates[37,38] had been successful before) was based on the electrochemical reduction of $HAuCl_4$ in the presence of 'shape-inducing' cationic surfactants and other additives. These had been found empirically to favor rod formation and act as both the supporting electrolyte and stabilizer for the resulting cylindrical Au nanoparticles[39]. In the electrochemical method, the micellar system consists of two cationic surfactants: cetyltrimethylammonium bromide (CTAB) and the much more hydrophobic tetradecylammonium bromide (TDAB) or TOAB. The ratio between the surfactants controls the average aspect ratio of the Au nanorods. The synthesis works on a small scale and, although it is very difficult to carry out on a large scale, represents a landmark in terms of shape control.

Subsequently, Murphy and coworkers discovered reduction conditions that enable the entire synthesis of Au and Ag nanorods to be carried out directly in solution[30,40], with excellent aspect ratio control. The method uses preformed Ag or Au seeds on which additional metal is grown in solution by means of a mild reducing agent (ascorbic acid), in the

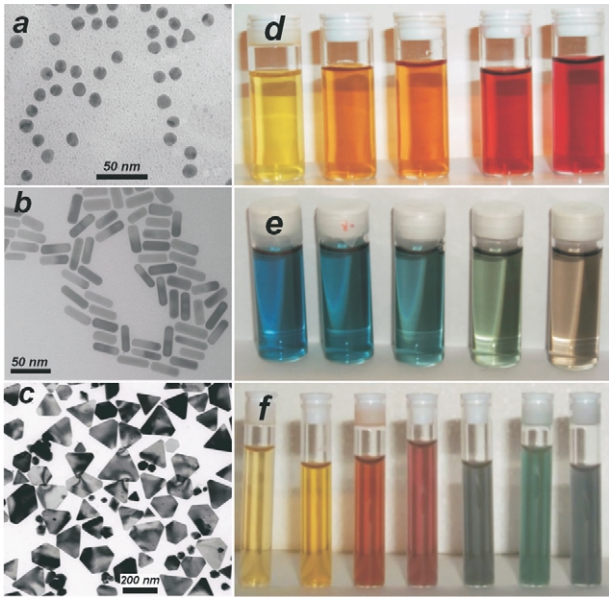

Fig. 1 Left: Transmission electron micrographs of Au nanospheres and nanorods (a,b) and Ag nanoprisms (c, mostly truncated triangles) formed using citrate reduction, seeded growth, and DMF reduction, respectively. Right: Photographs of colloidal dispersions of AuAg alloy nanoparticles with increasing Au concentration (d), Au nanorods of increasing aspect ratio (e), and Ag nanoprisms with increasing lateral size (f).

presence of CTAB to promote nanorod formation. The addition of different volumes of the seed solution produces Au nanorods with different aspect ratios. Recently, this method has been improved by El-Sayed and coworkers[31], resulting in a spectacular increase in the rod yield. Another modification of the method is based on a photochemical process[41] but, in contrast to the seed-mediated mechanism, the addition of a preformed Au seed is not needed. However, $AgNO_3$ is added to the growth solution containing CTAB and the Au salt before irradiating with ultraviolet light.

The controlled synthesis and optical characterization of metal nanoprisms was pioneered by Jin *et al.*[34], who converted citrate-stabilized Ag nanospheres into (truncated) triangular nanoprisms by irradiation with a fluorescent lamp in the presence of bis(p-sulfonatophenyl) phenylphosphine. The optical spectra of the nanoprisms display bands for in-plane dipole resonance, as well as for in-plane and out-of-plane quadrupole resonances, while the out-of-plane dipole is only reflected as a small shoulder.

Truncated Ag triangles have also been obtained by Chen and Carroll[35] using a procedure similar to the seeded growth method described for Au nanorod formation. In this case, the reduction was performed using ascorbic acid to reduce Ag ions on Ag seeds in a basic solution of concentrated CTAB. Malikova *et al.*[32] synthesized Au nanoprisms in aqueous solution by reduction of neutralized $HAuCl_4$ with salicylic acid at 80°C. Although the yield of nanoprisms was not outstanding, the formation of a thin film shows that strong optical coupling occurs when the nanoprisms are close enough to each other.

The mechanisms involved in the synthesis of spherical metal nanoparticles are well understood in general, but those leading to preferential growth in one particular direction are still the subject of debate. Evidence for an aggregative mechanism in some cases has been presented[28,42], but it is clear that such a mechanism does not apply in others. Further work in this direction is still needed.

Examples of metal nanoparticles with various shapes and sizes, together with dispersions of varying colors arising from different effects, are shown in Fig. 1.

Optical properties

The optical properties of small metal nanoparticles are dominated by the collective oscillation of conduction electrons resulting from the interaction with electromagnetic radiation. These properties are mainly observed in Au, Ag, and Cu, because of the presence of free conduction electrons. The electric field of the incoming radiation induces the formation of a dipole in the nanoparticle. A restoring force in the nanoparticle tries to compensate for this, resulting in a unique resonance wavelength (Fig. 2, top)[43].

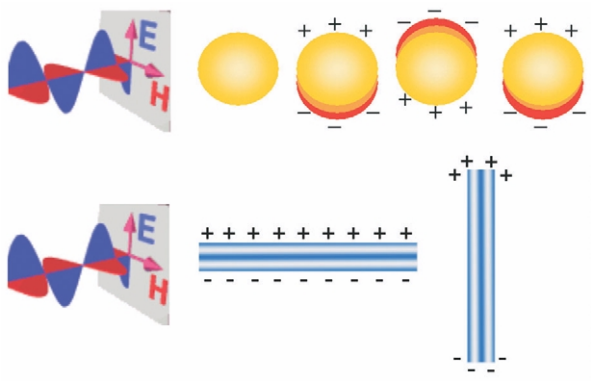

Fig. 2 (Top) Schematic drawing of the interaction of an electromagnetic radiation with a metal nanosphere. A dipole is induced, which oscillates in phase with the electric field of the incoming light. (Bottom) Transverse and longitudinal oscillation of electrons in a metal nanorod.

The oscillation wavelength depends on a number of factors, among which particle size and shape, as well as the nature of the surrounding medium, are the most important[5]. For nonspherical particles, such as rods, the resonance wavelength depends on the orientation of the electric field. Therefore, two oscillations, transverse and longitudinal, are possible (Fig. 2, bottom). In addition, when nanoparticles are sufficiently close together, interactions between neighboring particles arise, so that the models for isolated particles do not hold. The properties of dilute dispersions will be briefly discussed first, while a simple effective medium theory (Maxwell-Garnett) will be described next to account for the behavior of more concentrated systems, such as close-packed thin films.

Dilute Dispersions

The optical properties of dispersions of spherical particles with a radius R can be predicted by Mie theory[44], through expressions for the extinction cross section C_{ext}. For very small particles with a frequency dependent, complex dielectric function, $\varepsilon = \varepsilon' + i\varepsilon''$, embedded in a medium of dielectric constant ε_m, this can be expressed as:

$$C_{ext} = \frac{24\pi^2 R^3 \varepsilon_m^{3/2}}{\lambda} \frac{\varepsilon''}{(\varepsilon' + 2\varepsilon_m)^2 + \varepsilon''^2} \quad (1)$$

The origin of the strong color changes displayed by small particles lies in the denominator of eq 1, which predicts the existence of an absorption peak when

$$\varepsilon' = -2\varepsilon_m \quad (2)$$

In a small metal particle, the dipole created by the electric field of light induces a surface polarization charge, which effectively acts as a restoring force for the free electrons. The net result is that, when condition (2) is fulfilled, the long wavelength absorption by the bulk metal is condensed into a single surface plasmon band.

To calculate the spectra of elongated particles (nanorods), the orientation with respect to the oscillating electric field must be taken into account. The corresponding expression was derived by Gans[45]:

$$C_{ext} = \frac{8\pi^2 R^3 \varepsilon_m^{3/2}}{3\lambda} \sum_j \frac{\left(1/P_j^2\right)\varepsilon''}{\left(\varepsilon' + \frac{1-P_j}{P_j}\varepsilon_m\right)^2 + \varepsilon''^2} \quad (3)$$

where P_j represents the depolarization factors for the nanorod axes ($a > b = c$), which are defined as

$$P_a = \frac{1-r^2}{r^2}\left[\frac{1}{2r} ln\left(\frac{1+r}{1-r}\right) - 1\right];\ P_b = P_c = \frac{1-P_a}{2} \quad (4)$$

and the parameter r is related to the aspect ratio ($r = \sqrt{1 - (b/a)^2}$). Using these equations, El-Sayed and coworkers[46] derived an empirical relationship between the aspect ratio and the wavelength λ_{max} of the longitudinal plasmon resonance:

$$\lambda_{max} = 33.34\varepsilon_m \frac{b}{a} - 46.31\varepsilon_m + 472.31 \quad (5)$$

These expressions predict very well the colors shown in Figs. 1d and 1e. For other geometries, Mie theory has not yet been properly implemented, but different approaches have been devised, such as the discrete dipole approximation, which has been applied to the calculation of the spectra of Ag nanoprisms[34].

Thin Films

When the metal nanoparticle volume fraction is high, the equations above are no longer valid, since dipole-dipole interactions between neighboring nanoparticles are present, i.e. the oscillating dipoles of neighboring particles influence the frequency of a central particle. Under these conditions, effective medium theories are the simplest way to describe the optical response of the system. Such theories provide us with expressions to calculate the effective dielectric constant of the composite material, which can then be used to determine the corresponding absorption and reflection coefficients.

Among the various effective medium theories available, it has been found[7] that the one devised by Maxwell-Garnett[47] is suitable to describe these dipole-dipole interactions. Through the average polarization of the nanoparticles and the surrounding medium, the average dielectric function, $\varepsilon_{av} = (n_{av} + ik_{av})^2$, is calculated as

$$\varepsilon_{av} = \varepsilon_m \frac{\varepsilon(1+2\phi) + 2\varepsilon_m(1-\phi)}{\varepsilon(1-\phi) + \varepsilon_m(2+\phi)} \quad (6)$$

where ϕ is the metal volume fraction, ε_m is the dielectric function of the surrounding medium, and ε is the complex dielectric function of the nanoparticles. The transmittance, T, of radiation with a frequency ω through the film can be then calculated:

$$T_{film} = \frac{(1-R)^2 + 4R\sin^2\psi}{R^2 exp(-\alpha h) + exp(\alpha h) - 2R\cos(\zeta + 2\psi)} \quad (7)$$

where h is the film thickness, R is the reflectance at normal incidence,

$$R = \frac{(n_{av}-1)^2 + k_{av}^2}{(n_{av}-1)^2 + k_{av}^2} \quad (8)$$

and α is the absorption coefficient, which can be calculated from $\omega \mathrm{Im}(\varepsilon_{av})/cn_{av}$. Finally, we define the parameters $\zeta = 4\pi n_{av} h/\lambda$ and $\psi = \tan^{-1}(2k_{av}/(n_{av}^2 + k_{av}^2 - 1)$. Since eq 7 takes into account the reflection losses, it can be considered as the extinction coefficient of the film.

As an example of the absorption and reflection colors of thin films built up via layer-by-layer assembly[48] (using a positively charged polyelectrolyte as a molecular glue), Fig. 3 shows 15 nm Au nanoparticles surrounded with inert SiO_2 shells of varying thickness[7]. The absorption colors range from blue (the color of a thin, bulk film) for densely packed metal spheres to light red for well separated particles. The typical

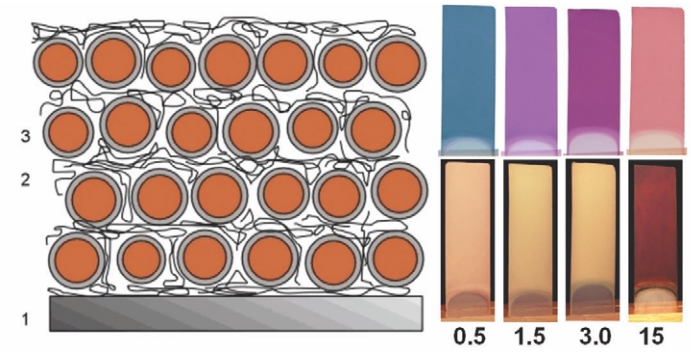

Fig. 3 Left: Schematic drawing of a multilayer film formed by layer-by-layer assembly of SiO_2-coated Au nanoparticles (1 = glass substrate; 2 = cationic polyelectrolyte; 3 = nanoparticles). Right: Photographs of transmitted (top) and reflected (bottom) colors from Au@SiO_2 multilayer thin films with varying silica shell thickness.

golden reflection is gradually lost as the particles are separated from each other.

Conclusion

Apart from the (linear) optical properties described here, nonlinear optical properties are also of great interest for applications of metal nanoparticles in ultrafast optical switches[49]. In particular, the third-order susceptibility of metal nanoparticles at wavelengths around the plasmon resonance achieves large values with very fast (<1 ps) response times. This is a consequence of the relaxation of the nonequilibrium electron distribution generated in the metal nanoparticles[50,51]. Theoretical and experimental studies taking into account the nature of the surrounding medium, interparticle interactions, and shape effects are still in their infancy and need much further attention. MT

Acknowledgments

I wish to acknowledge Jorge Pérez-Juste, Isabel Pastoriza-Santos, and Benito Rodríguez-González for providing unpublished figures, and Paul Mulvaney for having injected me with metal nanoparticle fever.

REFERENCES

1. www.thebritishmuseum.ac.uk/science/text/lycurgus/sr-lycurgus-p1-t.html
2. Faraday, M., *Philos. Trans. Royal Soc. London* (1857) **147**, 145
3. Kreibig, U., and Vollmer, M., *Optical Properties of Metal Clusters*, Springer-Verlag, Berlin (1996)
4. Link, S., and El-Sayed, M. A., *J. Phys. Chem. B* (1999) **103**, 8410
5. Mulvaney, P., *Langmuir* (1996) **12**, 788
6. Underwood, S., and Mulvaney, P., *Langmuir* (1994) **10**, 3427
7. Ung, T., *et al., J. Phys. Chem. B* (2001) **105**, 3441
8. Turkevich, J., *et al., Discuss. Faraday Soc.* (1951) **11**, 55
9. Frens, G., *Nature Physical Science* (1973) **241**, 20
10. A movie showing the procedure for synthesis of colloidal gold can be found at www.mrsec.wisc.edu/edetc/cineplex/gold/index.html
11. Turkevich, J., *et al., J. Phys. Chem.* (1986) **90**, 4765
12. Furlong, D. N., *et al., J. Chem. Soc., Faraday Trans. 1* (1984) **80**, 571
13. Brust, M., *et al., Chem. Comm.* (1994), 801
14. Brust, M., *et al., Chem. Comm.* (1995), 1655
15. Heath, J. R., *et al., J. Phys. Chem. B* (1997) **101**, 189
16. Korgel, B. A., *et al., J. Phys. Chem. B* (1998) **102**, 8379
17. Hostetler, M. J., *et al., J. Am. Chem. Soc.* (1996) **118**, 4212
18. Templeton, A. C., *et al., J. Am. Chem. Soc.* (1999) **121**, 7081
19. Hirai, H., *et al., J. Macromol. Sci., Chem.* (1979) **13**, 727
20. Wang, Y., and Toshima, N., *J. Phys. Chem. B* (1997) **101**, 5301
21. Ducamp-Sanguesa, C., *et al., J. Solid State Chem.* (1992) **100**, 272
22. Silvert, P.-Y., *et al., J. Mater. Chem.* (1996) **6**, 573
23. Sun, Y., *et al., Nano Lett.* (2002) **2**, 165
24. Sun, Y., *et al., Chem. Mater.* (2002) **14**, 4736
25. Pastoriza-Santos, I., and Liz-Marzán, L. M., *Langmuir* (2002) **18**, 2888
26. Pastoriza-Santos, I., and Liz-Marzán, L. M., *Langmuir* (1999) **15**, 948
27. Pastoriza-Santos, I., *et al., Langmuir* (2000) **16**, 2731
28. Giersig, M., *et al., J. Mater. Chem.*, in press (DOI:10.1039/B311454F)
29. Pastoriza-Santos, I., and Liz-Marzán, L. M., *Nano Lett.* (2002) **2**, 903
30. Jana, N. R., *et al., J. Phys. Chem. B* (2001) **105**, 4065
31. Nikoobakht, B., and El-Sayed, M. A., *Chem. Mater.* (2003) **15**, 1957
32. Malikova, N., *et al., Langmuir* (2002) **18**, 3694
33. Sanyal, A., and Sastry, M., *Chem. Comm.* (2003) **11**, 1236
34. Jin, R., *et al., Science* (2001) **294**, 1901
35. Chen, S., and Carroll, D. L., *Nano Lett.* (2002) **2**, 1003
36. Maillard, M., *et al., J. Phys. Chem. B* (2003) **107**, 2466
37. Martin, C. R., *Science* (1994) **266**, 1961
38. Schonenberger, C., *et al., J. Phys. Chem. B* (1997) **101**, 5497
39. Yu, Y.-Y., *et al., J. Phys. Chem. B* (1997) **101**, 6661
40. Murphy, C. J., and Jana, N. R., *Adv. Mater.* (2002) **14** (1), 80
41. Kim, F., *et al., J. Am. Chem. Soc.* (2002) **124**, 14316
42. Viau, G., *et al., Chem. Comm.* (2003) **17**, 2216
43. Henglein, A., *J. Phys. Chem.* (1993) **97**, 5457
44. Bohren, C. F., and Huffman, D. F., *Absorption and Scattering of Light by Small Particles*, Wiley, New York, (1983)
45. Gans, R., *Ann. Phys.* (1915) **47**, 270
46. Link, S., *et al., J. Phys. Chem. B* (1999) **103**, 3073
47. Maxwell-Garnett, J. C., *Philos. Trans. R. Soc. London* (1904) **203**, 385
48. Kotov, N. A., *et al., J. Phys. Chem.* (1995) **99**, 13065
49. Hache, F., *et al., J. Opt. Soc. Am. B* (1986) **3** (12), 1647
50. Tokizaki, T., *et al., Appl. Phys. Lett.* (1994) **65**, 941
51. Selvan, S. T., *et al., J. Phys. Chem. B* (2002) **106**, 10157